Research Square

Preprints are preliminary reports that have not undergone peer review.
They should not be considered conclusive, used to inform clinical practice,
or referenced by the media as validated information.

Climate-zone-dependent temperature sensitivity of Japanese encephalitis and the reversal of its age identity in China: a two-stage distributed lag non-linear analysis of six provinces, 2005–2020

Fei Wang
The First Affiliated Hospital of Xi'an Jiaotong University
Minghui Tai
The First Affiliated Hospital of Xi'an Jiaotong University
Mi Ke
The First Affiliated Hospital of Xi'an Jiaotong University
Yuxin Liu
The First Affiliated Hospital of Xi'an Jiaotong University
Yuanyuan Duan
Xi'an Center for Disease Control and Prevention
Tianyan Chen
The First Affiliated Hospital of Xi'an Jiaotong University
Zhen Tian
tianzhen@xjtufh.edu.cn

The First Affiliated Hospital of Xi'an Jiaotong University

Research Article

Keywords: Japanese encephalitis, climate, temperature, distributed lag non-linear model, two-stage meta-analysis, age structure, adult vaccination, China

Posted Date: October 22nd, 2026

DOI: https://doi.org/10.21203/rs.3.rs-11229651/v1

License: This work is licensed under a Creative Commons Attribution 4.0 International License.
Read Full License

Additional Declarations: No competing interests reported.

Abstract

Background

Japanese encephalitis (JE) has declined sharply in China since the vaccine entered the national Expanded Program on Immunization (EPI) in 2008, yet in northwestern provinces the disease has shifted from childhood to adult and elderly cases. Whether meteorological drivers differ by age group or climate zone remains untested in a multi-province, age-stratified framework.

Methods

We analysed monthly JE cases and deaths from six provinces spanning 21–38°N (Guizhou, Sichuan, Henan, Yunnan, Shaanxi, Gansu), 2005–2020, in three age bands (0–14, 15–59 and ≥ 60 years). Provincial population-weighted monthly temperature series were built from 166 stations, with denominators interpolated from the 2000, 2010 and 2020 censuses. Stage one fitted quasi-Poisson distributed lag non-linear models (monthly mean temperature, lag 0–2 months) to 18 province-by-band series, 16 with ≥ 50 cases; stage two pooled within age bands by random-effects meta-analysis and regressed the contrasts on latitude, childhood case share and annual mean temperature. Six sensitivity specifications, MDE, CFR decomposition and leave-one-outbreak-out analyses were performed.

Results

Among 22,875 cases (1,085 deaths), the age spectrum ran from childhood-dominated Guizhou (96.1% of cases aged 0–14 years) to adult-dominated Gansu (17.6%). The temperature–incidence relationship was threshold-shaped in all 16 series: flat below 12–14°C, rising steeply above 15°C. Pooled cumulative relative risks (90th vs 50th provincial temperature percentile) were 208.7 (95% CI 61.6–706.7), 164.0 (43.1–623.3) and 287.5 (4.6–17,800.6) for ages 0–14, 15–59 and ≥ 60 years, with no between-band difference ($P \geq 0.73$). Sensitivity increased with latitude (β = 0.228 log-RR per °N; $P = 0.005$) but not with childhood case share ($P = 0.60$), and was stable across all six sensitivity specifications; only 20- to 68-fold differences were detectable. CFR was two- to five-fold higher in the elderly; Gansu's CFR rose to 9.28% in 2017–2020, and 94% of the Gansu–Shaanxi gap reflected age-specific rates rather than age structure.

Conclusions

Temperature is a strong, threshold-shaped, latitude-graded driver of JE across six Chinese provinces but acts uniformly across age groups. The reversal of JE's age identity is therefore better explained by cohort immunity than by age-differential climate sensitivity, supporting adult catch-up vaccination in temperate zones such as southeastern Gansu.

Background

Japanese encephalitis (JE) is a mosquito-borne zoonosis maintained in a *Culex tritaeniorhynchus*–pig cycle [1] and remains the leading cause of viral encephalitis in Asia. China historically accounted for the majority of the global JE burden. After the live-attenuated JE vaccine was included in the national Expanded Program on Immunization (EPI) in 2008 [2], reported incidence fell to historically low levels, with 205, 125 and 128 cases reported nationally in 2023, 2024 and 2025, respectively [3].

Beneath this success, the age identity of the disease has reversed. National surveillance analyses show that 64% of JE cases in 2018 were aged ≥ 40 years, rising to 82% in northern low-endemicity provinces [4], and the Chinese Center for Disease Control and Prevention now describes the age distribution of JE as shifting towards adults [3]. The emblematic event was the 2017–2018 outbreak in Gansu Province, the largest since 1958: adults aged ≥ 20 years, predominantly rural farmers born before the EPI era, formed the case body, seropositivity declined with age, and no child cases were reported during the outbreak years [5, 6, 7]. In 2019 Gansu conducted a provincially funded catch-up campaign targeting rural residents aged 40–74 years in six key prefectures, achieving 99.4% coverage of the funded target population, and reported cases fell by 90.1% in 2019 [8]. The introduction of childhood JE vaccination through the EPI in 2008 has itself been assessed by quantitative analysis of national vaccine strategies from 1961 to 2020 [2] and, for Gansu Province specifically, by interrupted time-series analysis [9]. The effectiveness of the 2019 campaign, however, has only been reported administratively and has never been formally evaluated with adjustment for meteorological confounding.

That meteorological conditions drive JE is not in doubt: temperature, precipitation and humidity have repeatedly been associated with JE incidence, with non-linear thresholds and lags of weeks to months, as documented in southwestern China [10], in areas located near the Three Gorges Dam [11], in Shaanxi [12] and in wider analyses of prevalence dynamics [13]; ongoing changes in climate and weather are expected to alter vector-borne disease transmission more broadly [14]. However, every published analysis to date is a single-city or single-province descriptive study; none has pooled estimates across provinces, stratified by age, at monthly resolution, or tested whether exposure–response gradients differ along a climate-zone gradient. In particular, no study has asked the question central to the age-reversal phenomenon: do older, largely unvaccinated cohorts in temperate provinces show stronger meteorological sensitivity than the EPI-covered child populations of subtropical provinces?

We therefore conducted a two-stage distributed lag non-linear analysis of monthly, age-stratified JE surveillance data from six provinces spanning 21–38°N, 2005–2020, with three objectives: (i) to characterise the temperature–incidence relationship by province and age band; (ii) to test formally whether temperature sensitivity differs between age bands and along the climate-zone gradient; and (iii) to quantify the fatality burden associated with the age reversal, thereby clarifying whether that reversal is a meteorological-sensitivity phenomenon or a cohort-immunity phenomenon.

Methods

Study design and setting

We conducted a province-by-month-by-age-band ecological time-series study covering 2005–2020. Six provinces were selected a priori on three criteria: historically high JE burden; joint coverage of the 21–38°N climate gradient; and coverage of both ends of the age-spectrum transition. The selected provinces (Guizhou, Sichuan, Henan, Yunnan, Shaanxi, Gansu) form a southwestern to northwestern transect across the major JE endemic belt.

Case and death data

Monthly counts of JE cases and deaths by 27 age groups (single years 0–9; five-year groups 10–14 to 80–84; ≥85 years; and unknown) were obtained from the national notifiable disease surveillance system for the six provinces, January 2005 to December 2020. Quality control covered 48 indicators; a single case had unknown age and was excluded from age-specific analysis. In 53 province-months, recorded deaths exceeded recorded cases; these reflect registration-month misalignment and were retained because period totals are unaffected. Age groups were collapsed into three EPI-eligibility-aligned bands: 0–14, 15–59 and ≥ 60 years.

Meteorological data

Daily ground-station records (mean, maximum and minimum temperature; relative humidity; 20–20 h precipitation) were drawn from the China Meteorological Administration daily climate dataset (V3.0). Of 609 stations screened, 166 met the eligibility criteria (at least 95% daily coverage over 2005–2020 before gap-filling and at least 99.5% after short gaps were filled from the nearest neighbouring station; median fill rate 0.02%). Station-relocation artefacts were screened using recorded latitude and altitude discontinuities. Provincial monthly exposure series were constructed by population weighting: each station was weighted by its prefecture population (2020 census) divided by the number of eligible stations in that prefecture, so that the exposure series represents the population rather than the station network. Equal-weight station averages were retained for sensitivity analyses. Population weighting materially corrected exposure in mountainous provinces (for example, Sichuan July mean temperature changed from 20.3°C to 25.4°C).

Population denominators

Monthly province-by-age-band populations were interpolated from the 2000, 2010 and 2020 census age pyramids: totals were interpolated geometrically and age composition linearly, anchored exactly at the census reference dates (November 2000, November 2010 and November 2020).

Statistical analysis

Stage one. For each of the 18 province-by-band series we fitted a quasi-Poisson generalised linear model of monthly cases on a cross-basis [15] of monthly mean temperature (natural cubic spline with knots at the 25th and 75th percentiles of the pooled temperature distribution; lag 0–2 months with a natural-spline lag structure), adjusting for relative humidity and precipitation (natural splines, 3 df each) and a natural-spline long-term trend (16 df over 16 years), with the log of monthly person-time as offset. Two series with fewer than 50 cases were excluded a priori (Guizhou ≥ 60 years, 7 cases; Sichuan ≥ 60 years, 41 cases), leaving 16 series for stage two. Full-year series were modelled: winter near-zero incidence anchors the low-temperature limb, whereas a transmission-season window produced unstable boundary behaviour in sparse series. Two series that failed to converge owing to separation (Shaanxi 0–14 years; Henan ≥ 60 years) were fitted with Firth-penalised Poisson regression, with the variance–covariance matrix rescaled by the Pearson dispersion.

Stage two. Within each age band, cross-basis coefficients were pooled by multivariate meta-analysis [16] (random effects with diagonal between-series covariance, or fixed effects when the random-effects model was not identifiable), and the pooled cumulative exposure–response curve was evaluated over the intersection of the member-series temperature ranges. The headline estimand was the cumulative relative risk (RR) comparing each series' own 90th versus 50th temperature percentile — a within-province percentile contrast that is comparable across climate zones — pooled by univariate random-effects meta-analysis within each band, following the two-stage design used in multi-city temperature–health studies [17]. Between-band differences were tested by meta-regression on the band indicator with Wald tests.

Meta-regression on province-level covariates. To explain between-province heterogeneity, the per-series log-RR contrasts were regressed (band-adjusted) on three pre-specified covariates: the provincial share of cases aged 0–14 years (the age-identity axis), the mean latitude of eligible stations (the climate-zone axis), and annual mean temperature.

Sensitivity and robustness. Six specifications were compared: (i) the main analysis; (ii) equal-weight station exposure; (iii) exclusion of 2020 (COVID-19 perturbation); (iv) minimum temperature as the exposure; (v) a conservative calendar-month fixed-effect design, in which identification comes from within-month interannual anomalies and the estimand is the RR per 1°C anomaly; and (vi) a year-indicator trend in place of the spline trend. A leave-one-outbreak-out analysis excluded Gansu 2018. Because the between-band tests were negative, we computed the minimum detectable effect (MDE; 80% power, two-sided $\alpha = 0.05$) for each pairwise band contrast from the meta-regression variance–covariance matrix.

Fatality burden. Province- and band-specific CFRs with Wilson confidence intervals were computed, CFR trends were described over four calendar periods, and the Gansu–Shaanxi CFR gap was decomposed into age-composition and age-specific-rate components (Kitagawa decomposition) with direct standardisation to the pooled case age structure.

Analyses were performed in R version 4.6.1 (packages *dlnm*, *mvmeta*, *brglm2*) and Python version 3.12.

Results

Descriptive epidemiology: a continuous age-spectrum transect

The six provinces reported 22,875 JE cases and 1,085 deaths (overall CFR 4.7%) during 2005–2020 (Table 1, Fig. 1). The share of cases aged 0–14 years decreased monotonically along the transect: 96.1% in Guizhou, 94.8% in Sichuan, 79.4% in Henan, 69.1% in Yunnan, 39.7% in Shaanxi and 17.6% in Gansu, while the share aged ≥ 60 years rose from 0.1% to 31.3%. Population-denominator incidence quantified the same gradient: mean monthly crude incidence in children aged 0–14 years was 0.277, 0.201 and 0.165 per 100,000 population in Guizhou, Sichuan and Yunnan, whereas incidence in adults aged ≥ 60 years reached 0.073 and 0.049 per 100,000 population in Gansu and Shaanxi. The southwestern provinces peaked in 2006–2007 and declined monotonically after EPI introduction; Gansu instead showed an independent adult-outbreak peak in 2018 (503 cases) (Fig. 1).

Table 1
JE cases, deaths, case-fatality ratio and age composition by province, 2005–2020

Province	Cases	Deaths	CFR (%)	0–14 year (%)	≥ 60 year (%)	Peak year (cases)
Guizhou	5,059	268	5.3	96.1	0.1	2006 (1,519)
Sichuan	5,736	215	3.7	94.8	0.7	2006 (1,199)
Henan	4,132	189	4.6	79.4	7.6	2006 (876)
Yunnan	4,406	219	5.0	69.1	2.9	2007 (759)
Shaanxi	2,005	70	3.5	39.7	25.7	2006 (504)
Gansu	1,537	124	8.1	17.6	31.3	2018 (503)
Total	22,875	1,085	4.7	–	–	–

Provinces are ordered by decreasing share of cases aged 0–14 years. CFR, case-fatality ratio; yr, years.

Stage one: a consistent threshold-shaped temperature response

Sixteen of the 18 series entered stage two. Despite spanning 21–38°N, the cumulative exposure–response curves were qualitatively consistent across provinces and age bands (Fig. 2): risk was flat and near baseline below approximately 12–14°C, then rose steeply and approximately log-linearly above about 15°C. Because JE incidence is near zero in winter, the dynamic range of the fitted response is large; all curves are therefore presented on the logarithmic scale.

Stage two: strong temperature effects, no age-band gradient

Pooled cumulative RRs comparing the provincial 90th versus 50th temperature percentile (lags 0–2 months) were 208.7 (95% CI 61.6–706.7) for ages 0–14 years, 164.0 (95% CI 43.1–623.3) for ages 15–59 years and 287.5 (95% CI 4.6–17,800.6) for ages ≥ 60 years (Table 2, Fig. 3). Between-band differences were small and non-significant (pairwise Wald $P = 0.73–1.00$). The conservative calendar-month specification, identified purely from within-month temperature anomalies, yielded significant and mutually similar effects in all bands (RR per 1°C anomaly: 2.10, 1.92 and 2.54, respectively; pairwise $P \geq 0.44$).

Table 2
Pooled cumulative RR (provincial 90th vs 50th temperature percentile, lags 0–2 months) by age band, main and sensitivity analyses

Specification	Age 0–14	Age 15–59	Age ≥ 60	Band *P*
Main (population-weighted Tmean)	208.7 (61.6–706.7)	164.0 (43.1–623.3)	287.5 (4.6–17,800.6)	≥ 0.73
Equal-weight stations	188.5 (75.4–471.3)	157.7 (37.7–658.8)	170.1 (1.6–18,653.8)	≥ 0.57
Excluding 2020	176.3 (56.6–549.4)	151.1 (37.6–607.2)	455.3 (1.8–115,537.2)	≥ 0.77
Minimum temperature	199.1 (73.6–538.9)	135.1 (44.7–408.0)	347.7 (12.6–9,577.9)	≥ 0.57
Calendar-month FE (per 1°C anomaly)	2.10 (1.37–3.21)	1.92 (1.27–2.89)	2.54 (1.20–5.38)	≥ 0.44
Year-indicator trend	184.8 (54.2–630.3)	135.8 (40.6–454.5)	388.8 (5.7–26,719.1)	≥ 0.71
Gansu 2018 left out	198.4 (59.6–660.6)	171.2 (43.5–672.7)	850.5 (3.8–189,280.6)	≥ 0.79

* Smallest pairwise Wald P-value among the three band contrasts. RRs are on the natural scale; the calendar-month specification is per 1°C within-month anomaly. CIs are 95%. FE, fixed effects; Tmean, mean temperature.

Meta-regression: latitude, not age structure, modifies temperature sensitivity

Band-adjusted meta-regression of the 15 informative series showed that temperature sensitivity increased significantly with latitude (β = 0.228 log-RR per °N; $z = 2.81$; $P = 0.005$): the seasonal amplification of JE risk per degree of warming is systematically stronger in the temperate northwest (Table 3). Neither the provincial share of childhood cases (β = −0.010 per percentage point; $P = 0.60$) nor annual mean temperature (β = −0.266 per °C; $P = 0.16$; highly collinear with latitude) explained the

heterogeneity. Residual between-series heterogeneity was negligible (I^2 = 0%), indicating that the contrast-specific variance dominates.

Table 3
Band-adjusted meta-regression of temperature-sensitivity contrasts on province-level covariates, and minimum detectable effects for band differences

Covariate / contrast	**β or log-RR difference**	***z***	***P***
Childhood case share (per 1%)	−0.010	−0.53	0.60
Latitude (per 1 °N)	0.228	2.81	0.005
Annual mean temperature (per 1°C)	−0.266	−1.39	0.16
MDE: 0–14 vs 15–59 (RR ratio)	20.5-fold	–	power 5.3% at observed 1.45
MDE: 0–14 vs ≥ 60 (RR ratio)	68.2-fold	–	power 4.4% at observed 1.46
MDE: 15–59 vs ≥ 60 (RR ratio)	60.7-fold	–	power 2.5% at observed 1.00
MDE, minimum detectable effect (80% power, two-sided α = 0.05).			

Robustness

Pooled estimates were essentially unchanged under equal-weight exposure (188.5 / 157.7 / 170.1 by band), exclusion of 2020 (176.3 / 151.1 / 455.3), minimum temperature as the exposure (199.1 / 135.1 / 347.7) and year-indicator trends (184.8 / 135.8 / 388.8); no between-band difference approached significance in any specification (all $P \geq 0.44$) (Table 2). Excluding the 2018 Gansu outbreak left the pooled childhood and adult estimates essentially unchanged (198.4 and 171.2 versus 208.7 and 164.0 in the main specification) but moved the already imprecise pooled elderly estimate upwards (850.5, 95% CI 3.8–189,280.6, versus 287.5) (Table 2). Within the Gansu series itself, the series-specific 0–14 and 15–59 year cumulative RRs moved from 947.2 and 187.3 to 847.7 and 245.7, and the Gansu ≥ 60-year estimate became uninformative, because its elderly signal derives largely from the outbreak years. We flag this as a limitation rather than as a contradiction.

A leave-one-province-out meta-regression examined the leverage of individual provinces on the province-level associations (Additional file 1: Table S1, leave-one-province-out meta-regression of the temperature-sensitivity contrast on province-level covariates; Fig. S1, forest plot of the latitude coefficient). The latitude gradient did not depend on the outbreak province: excluding Gansu strengthened rather than weakened the estimate (β = 0.280 log-RR per °N; P = 0.010), and exclusion of Guizhou, Henan, Shaanxi or Sichuan left it significant (β = 0.189–0.259; P = 0.001–0.041). Excluding Yunnan, however, attenuated the coefficient to null (β = −0.005; P = 0.96): without its subtropical anchor the across-province range of this covariate contracts from 25–37°N to 27–37°N, well inside the 21–38°N

span of the six provinces, and with only five provinces the gradient becomes uninformative. The latitude signal is therefore a property of the full north-south transect rather than of the temperate end alone — robust to the removal of any single temperate province, but necessarily dependent on the transect endpoints with six provinces. The null associations for childhood case share and annual mean temperature were unchanged in every leave-one-out run ($P \geq 0.36$ and $P \geq 0.057$, respectively).

Fatality burden and the age reversal

CFR rose steeply with age in every province, with elderly CFR roughly two- to five-fold the childhood CFR (for example, Sichuan: 17.1% at ≥ 60 years versus 3.7% at 0–14 years) (Fig. 4). Five provinces showed declining CFR over time, but Gansu's CFR rose from 4.40% in 2013–2016 to 9.28% in 2017–2020, coinciding with the adult outbreak. Gansu's crude CFR (8.07%) exceeded Shaanxi's (3.49%); direct standardisation reduced Gansu to 5.79%, and Kitagawa decomposition attributed 94% of the 4.58-percentage-point gap to province differences in age-specific fatality rates and only 6% to the older case age structure.

Minimum detectable effects

The design had 80% power to detect only 20.5-fold (0–14 versus 15–59 years), 68.2-fold (0–14 versus ≥ 60 years) and 60.7-fold (15–59 versus ≥ 60 years) RR ratios; power for the observed differences (ratios 1.00–1.46) was 2.5–5.3% (Table 3). The null between-band tests should therefore be read as an absence of evidence for large differences, with moderate differences undetectable at this sample size.

Discussion

In this six-province, age-stratified, monthly two-stage analysis — to our knowledge the first of its kind for JE — we found that (i) temperature is a strong, threshold-shaped driver of JE incidence across a 17-degree latitudinal transect; (ii) the strength of the temperature response does not differ materially between children, adults and the elderly; (iii) temperature sensitivity is instead graded by latitude, with steeper seasonal amplification in the temperate northwest; and (iv) the fatality burden of the age reversal is doubly amplified, because elderly cases are both more numerous in the northwest and intrinsically more likely to die.

The principal scientific implication concerns the mechanism of the age reversal. Had meteorological sensitivity been concentrated in unvaccinated adult cohorts — for example because outdoor agricultural exposure amplifies climate-driven transmission — the band-specific temperature responses should have diverged along the transect. They did not. Temperature acted essentially uniformly across age bands, while the age composition of cases varied by a factor of five between provinces. Together with the absence of child cases during the Gansu outbreak years and serological evidence that antibody positivity declines with age in the northwest [5] but rises with age in the south [20], our results support a cohort-immunity explanation: the age reversal tracks who is unvaccinated (pre-EPI birth cohorts), not who is climatically susceptible. Climate shapes where and when transmission intensifies; immunity profiles determine whom it affects.

The latitude gradient in temperature sensitivity is itself notable. The same percentile contrast produces a larger relative amplification in temperate provinces, plausibly because vector abundance and the viral extrinsic incubation period are closer to their thermal limits there, so that warm anomalies shift transmission more sharply. This implies that the temperate margins of the endemic belt — precisely where adult susceptibility concentrates — may be the most climate-sensitive JE terrain in China, an intersection that deserves targeted surveillance as warming proceeds.

Our findings on fatality carry a direct policy message. The two- to five-fold elderly CFR gradient means that every proportional shift of cases towards older ages multiplies the death burden, and the rise in Gansu's CFR during 2017–2020, unexplained by age structure alone (94% of the Gansu–Shaanxi gap was attributable to age-specific rates), suggests additional drivers such as delayed care-seeking, comorbidity or clinical-recognition gaps in a previously low-endemicity province. The 2019 Gansu catch-up campaign for rural adults aged 40–74 years (99.4% of the funded target population; cases down 90.1%; incidence 0.19 per 100,000) is the natural policy response. Recent randomised trial evidence that Japanese encephalitis vaccine schedules are immunogenic in adults aged 40–69 years supports its feasibility [18], complemented by population-based immunogenicity data covering a wider age range [19]. Yet the campaign's effectiveness has never been formally evaluated with meteorological adjustment; the distributed lag non-linear modelling framework assembled here provides the confounding control that such an evaluation requires.

Strengths of the study include the multi-province climate-transect design with pre-specified selection criteria; age-stratified monthly surveillance over 16 years; population-weighted exposure series that correct station-network bias in mountainous provinces; census-anchored monthly denominators; and an extensive robustness programme (six specifications, leave-one-outbreak-out and leave-one-province-out analyses, dispersion-rescaled variances for separated series, Firth fits, and MDE quantification).

Several limitations qualify the interpretation. First, the between-band null rests on limited power: the design could detect only 20-fold or larger RR ratios, and the elderly series in two provinces were too sparse to model at all (Guizhou and Sichuan, ≥ 60 years), leaving the ≥ 60-year pool to three or four provinces. Second, monthly resolution smooths within-month exposure variability and precludes fine lag resolution; our 0–2-month lag window, although standard for vector-borne diseases at monthly scale, cannot separate vector-development from human-incubation lags. Third, provincial exposure series aggregate substantial within-province climate heterogeneity (exemplified by the Sichuan basin–mountain contrast), biasing the exposure–response towards the population mean. Fourth, surveillance data are subject to under-ascertainment and to reporting changes, and the strong post-2008 decline in incidence, although controlled by flexible trend terms and by the year-indicator specification, may imperfectly separate vaccine effects from climatic trends. Fifth, province-reported vaccination coverage series were not available in a consistent form and were not modelled; the cohort-immunity interpretation therefore rests on case-composition and serological evidence rather than on coverage covariates. Sixth, with six provinces the province-level meta-regression is necessarily endpoint-sensitive: the latitude gradient survives removal of any single temperate province, including the outbreak province, but not

removal of the subtropical anchor, and should be read as a transect-level association rather than a locally identified dose–response. Finally, the ecological design precludes individual-level causal inference.

Future work should (i) formally evaluate the 2019 Gansu adult campaign with interrupted time-series designs adjusted by the meteorological framework developed here; (ii) extend the transect to additional temperate provinces to sharpen the latitude gradient and the elderly estimates; and (iii) integrate serological surveys into the meta-regression, replacing case-composition proxies of immunity with direct measurements.

Conclusions

Across six Chinese provinces spanning the JE climate gradient in 2005–2020, temperature showed a strong, threshold-shaped, latitude-graded association with JE incidence that was essentially uniform across age groups. The reversal of JE from a childhood to an adult disease is therefore not explained by age-differential climate sensitivity; it is a cohort-immunity phenomenon superimposed on a climate-driven transmission system. Because elderly cases carry a two- to five-fold higher fatality risk, adult catch-up vaccination in emerging temperate transmission zones — beginning with southeastern Gansu-type settings — is a priority, and the unevaluated 2019 Gansu campaign offers a unique natural experiment for measuring its effect.

Abbreviations

CFR
case-fatality ratio
CI
confidence interval
DLNM
distributed lag non-linear model
EPI
Expanded Program on Immunization
JE
Japanese encephalitis
MDE
minimum detectable effect
RR
relative risk.

Declarations

Ethics approval and consent to participate

Not applicable. The study used aggregated, de-identified surveillance counts and publicly available meteorological and census data; no individual-level data were accessed.

Consent for publication

Not applicable.

Clinical trial number

Clinical trial number: not applicable. This was an ecological analysis of routinely collected, aggregated surveillance data; no trial participants were enrolled, allocated, or followed up.

Availability of data and materials

The aggregated case data analysed in this study were obtained from the National Population Health Data Center (PHDA) notifiable infectious disease surveillance data repository (http://www.ncmi.cn); these data are available from the corresponding author on reasonable request. The meteorological data were obtained from the China Meteorological Administration SURF_CLI_CHN_MUL_DAY V3.0 dataset via the National Tibetan Plateau / Third Pole Environment Data Center (http://data.tpdc.ac.cn). The analysis datasets and code (R and Python) are available from the corresponding author on reasonable request.

Competing interests

The authors declare that they have no competing interests.

Funding

This work was supported by the Natural Science Basic Research Program Youth Project of the Shaanxi Provincial Science and Technology Department (No. 2023-JC-QN-0830). The funding body played no role in the design of the study and the collection, analysis, and interpretation of data, or in writing the manuscript.

Authors' contributions

FW, MT and ZT conceived and designed the study. FW, MT and YL acquired the surveillance, meteorological and census data and curated the analysis datasets. FW performed the statistical analysis and drafted the manuscript, with methodological support from MT and YL. MK and YL contributed to data validation, quality control and the literature review. YD contributed virological and surveillance expertise and assisted with acquisition and interpretation of the surveillance data. MT verified the underlying data and contributed to drafting and revision of the manuscript. TC and ZT supervised the study, contributed to the interpretation of the results and critically revised the manuscript for important intellectual content. ZT acquired the funding and is the guarantor of the work. FW and MT contributed equally to this work and share first authorship. All authors read and approved the final manuscript.

Acknowledgements

We thank the Data-center of China Public Health Science and the China Meteorological Data Sharing Service System for data access.

References

1. Liu XT, Jiang LD, Lin YT, Zhao R, Wang Q, Zhang SY, et al. Prevalence of Japanese encephalitis in pigs in Mainland China during 2000–2024: a systematic review and meta-analysis. Front Vet Sci. 2025;12:1534114. 10.3389/fvets.2025.1534114.
2. Shi T, Meng L, Li D, Zhao X, Zhang X, Liu Y, et al. Effect of different vaccine strategies for the control of Japanese encephalitis in mainland China from 1961 to 2020: a quantitative analysis. Vaccine. 2022;40:6243–54. 10.1016/j.vaccine.2022.09.030.
3. Chinese Center for Disease Control and Prevention. Japanese encephalitis: frequently asked questions. 2026. Available from: https://www.chinacdc.cn/jkyj/mygh02/ymkyfjb/yn/202606/t20260622_1837237.html. Accessed 30 September 2026.
4. Wu D, Chen X, Liu W, Fu S, Li F, Liang G, et al. Emergence of Japanese encephalitis among adults 40 years of age or older in northern China: epidemiological and clinical characteristics. Transbound Emerg Dis. 2021;68:3415–23. 10.1111/tbed.13945.
5. Zhang X, Jin N, Tu A, Dong M, Shi T, Ren X, et al. Adults in Northwest China experienced the largest outbreak of Japanese encephalitis in history 10 years after the Japanese encephalitis vaccine was included in the national immunization program: a retrospective epidemiological study. J Med Virol. 2023;95:e28782. 10.1002/jmv.28782.
6. Wang X, He A, Zhang C, Wang Y, An J, Zhang Y, et al. Japanese encephalitis transmission trends in Gansu, China: a time series predictive model based on spatial dispersion. One Health. 2023;16:100554. 10.1016/j.onehlt.2023.100554.
7. Jin N, Zhang XS, Dong MX, Zhang BL, Zhang NJ, Liu SY, et al. Spatial-temporal distribution of Japanese encephalitis in Gansu Province, 2005–2019. Zhongguo Yi Miao He Mian Yi. 2020;26:411–6. 10.19914/j.cjvi.2020.04.013. (In Chinese).
8. Gansu Provincial Health Commission. Notification on Japanese encephalitis prevention and control: results of the adult catch-up vaccination campaign, 25 October 2019. China Gansu Net. Available from: https://gansu.gscn.com.cn/system/2019/10/25/012251655.shtml. Accessed 30 September 2026. (In Chinese).
9. Shi TS, Meng L, Li DH, Zhang XS, Zhao XK, Jin N, et al. Evaluation of the impact of Japanese encephalitis vaccine included in the expanded immunization program on the reported incidence of Japanese encephalitis in Gansu province: an interrupted time series analysis. Zhonghua Liu Xing Bing Xue Za Zhi. 2022;43:1087–92. 10.3760/cma.j.cn112338-20211214-00980. (In Chinese).

10. Liu Z, Zhang Y, Tong MX, Zhang Y, Xiang J, Gao Q, et al. Nonlinear and threshold effect of meteorological factors on Japanese encephalitis transmission in Southwestern China. Am J Trop Med Hyg. 2020;103:2442–9. 10.4269/ajtmh.20-0040.
11. Bai Y, Xu Z, Zhang J, Mao D, Luo C, He Y, et al. Regional impact of climate on Japanese encephalitis in areas located near the three gorges dam. PLoS ONE. 2014;9:e84326. 10.1371/journal.pone.0084326.
12. Zhang S, Hu W, Qi X, Zhuang G. How socio-environmental factors are associated with Japanese encephalitis in Shaanxi, China — a Bayesian spatial analysis. Int J Environ Res Public Health. 2018;15:608. 10.3390/ijerph15040608.
13. Tu T, Xu K, Xu L, Gao Y, Zhou Y, He Y, et al. Association between meteorological factors and the prevalence dynamics of Japanese encephalitis. PLoS ONE. 2021;16:e0247980. 10.1371/journal.pone.0247980.
14. Fouque F, Reeder JC. Impact of past and on-going changes on climate and weather on vector-borne diseases transmission: a look at the evidence. Infect Dis Poverty. 2019;8:51. 10.1186/s40249-019-0565-1.
15. Gasparrini A, Armstrong B, Kenward MG. Distributed lag non-linear models. Stat Med. 2010;29:2224–34. 10.1002/sim.3940.
16. Gasparrini A, Armstrong B, Kenward MG. Multivariate meta-analysis for non-linear and other multi-parameter associations. Stat Med. 2012;31:3821–39. 10.1002/sim.5471.
17. Gasparrini A, Guo Y, Hashizume M, Lavigne E, Zanobetti A, Schwartz J, et al. Mortality risk attributable to high and low ambient temperature: a multicountry observational study. Lancet. 2015;386:369–75. 10.1016/S0140-6736(14)62114-0.
18. Wu D, Yin QK, Zhang Y, Li YX, Zhou LW, Fu SH, et al. Immunogenicity, immune persistence, and safety of Japanese encephalitis vaccine schedules among adults in Ningxia, China. NPJ Vaccines. 2025;10:222. 10.1038/s41541-025-01270-2.
19. Zhang Y, Zhou LP, Zhou Y, Liu W, Fu SH, Wang HY, et al. Immunogenicity of one dose of Japanese encephalitis attenuated live vaccine among 2–70-year-olds in north Ningxia Hui Autonomous Region. Zhongguo Yi Miao He Mian Yi. 2023;29:661–4. (In Chinese).
20. Chen Y, Yuan R, Qian Z, Li X, Lin W, Xiong C, et al. Unveiling immunity dynamics: serological characteristics of antibodies against Japanese encephalitis virus in Guangdong, China. PLoS Negl Trop Dis. 2025;19:e0013629. 10.1371/journal.pntd.0013629.

Figures

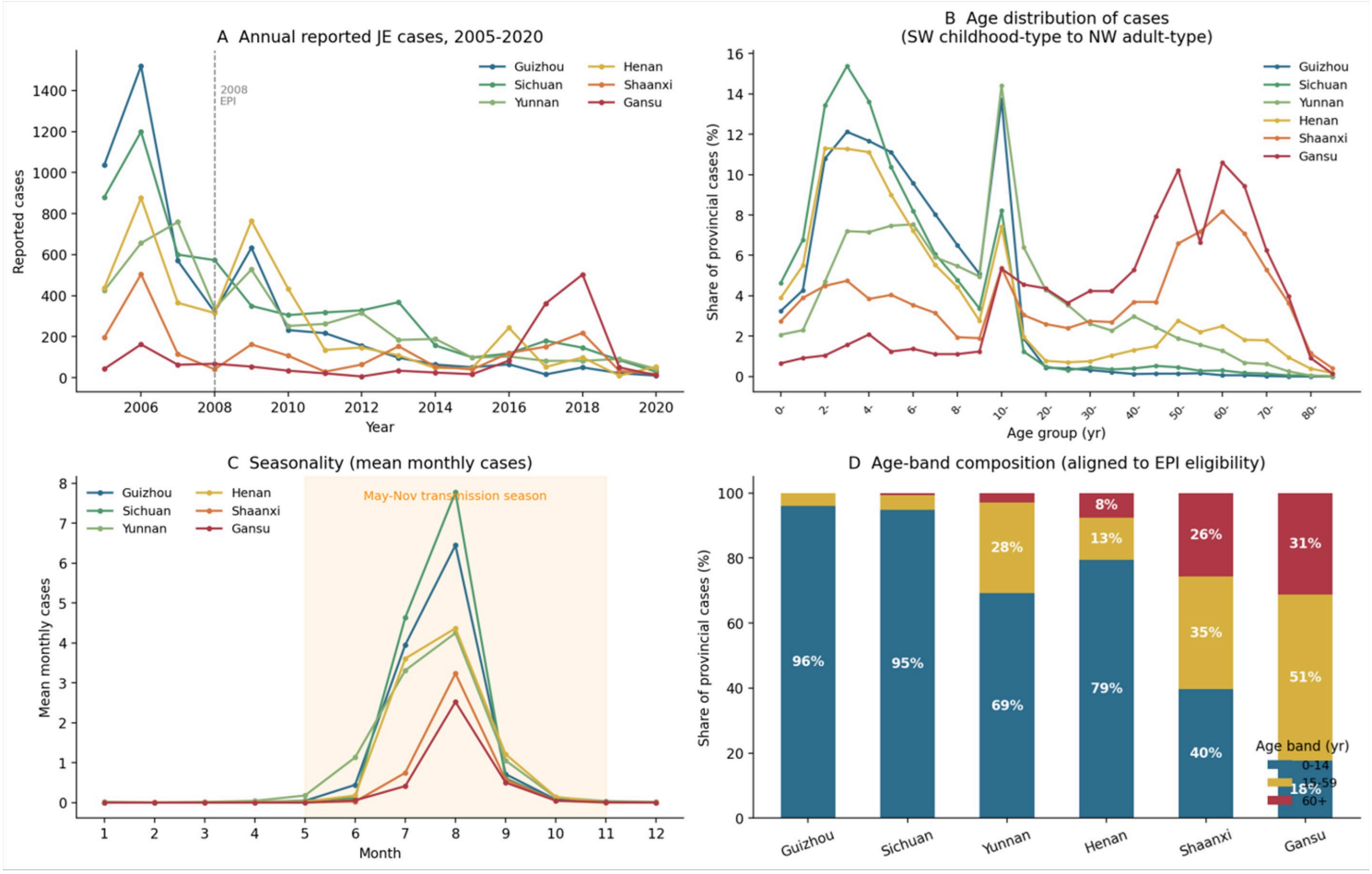


Figure 1

Epidemiological overview of JE in the six study provinces, 2005–2020.

(**A**) Annual reported cases; the dashed line marks EPI introduction (2008). (**B**) Age distribution of cases, showing the continuous spectrum from childhood-dominated southwestern to adult-dominated northwestern provinces. (**C**) Seasonality (mean monthly cases); shading indicates the May–November transmission season. (**D**) Age-band composition aligned to EPI eligibility.

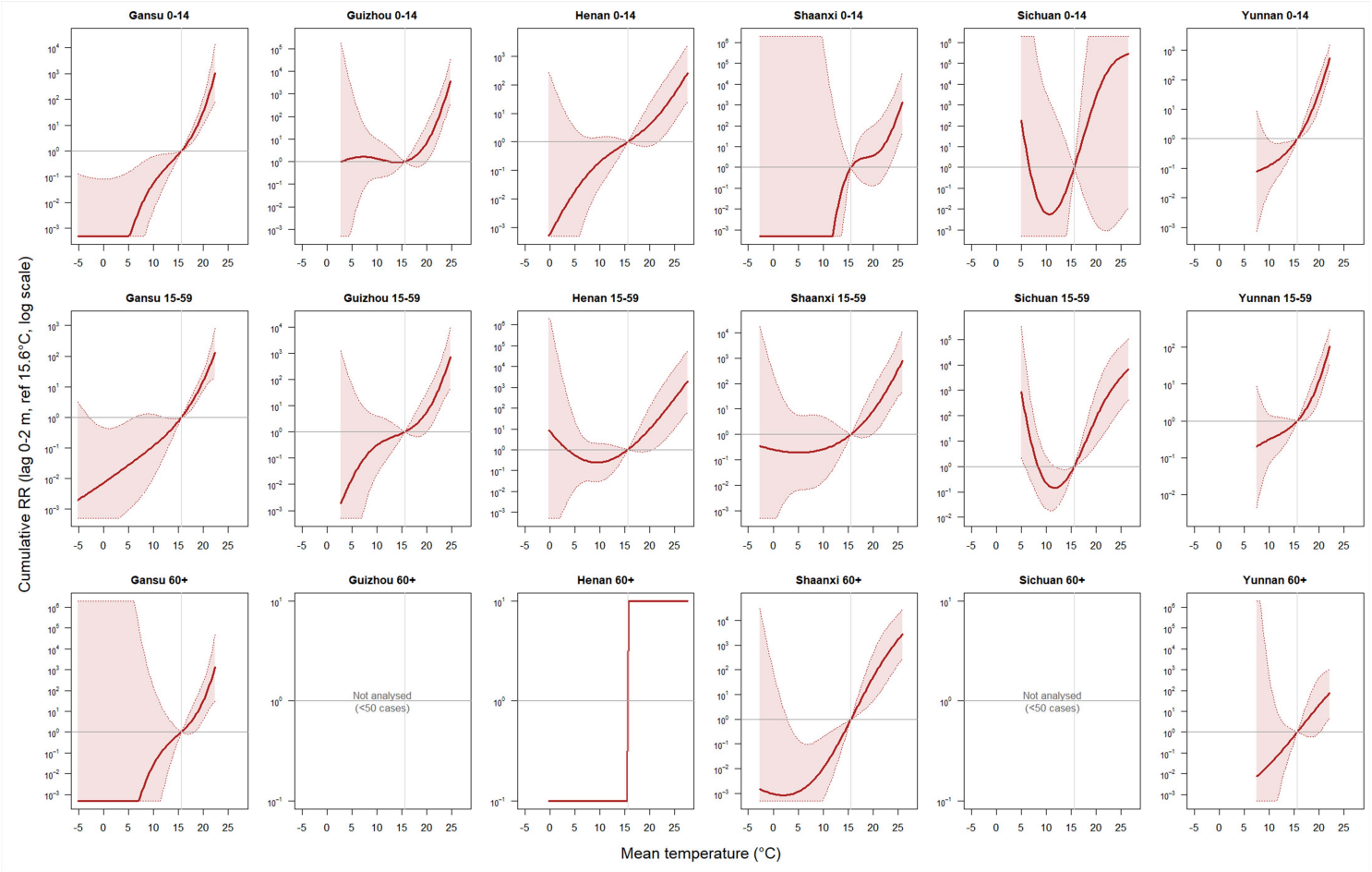


Figure 2

Stage-one cumulative exposure–response curves by province and age band.

Curves show the association between monthly mean temperature and JE incidence (lag 0–2 months, log scale) for the 16 province-by-age-band series, relative to the pooled median (15.6 °C); shading indicates 95% CIs. Series with fewer than 50 cases (Guizhou ≥60 years, Sichuan ≥60 years) were excluded a priori and appear as empty panels marked "Not analysed". Two series (Shaanxi 0–14 years and Henan ≥60 years) were fitted with Firth-penalised regression owing to separation.

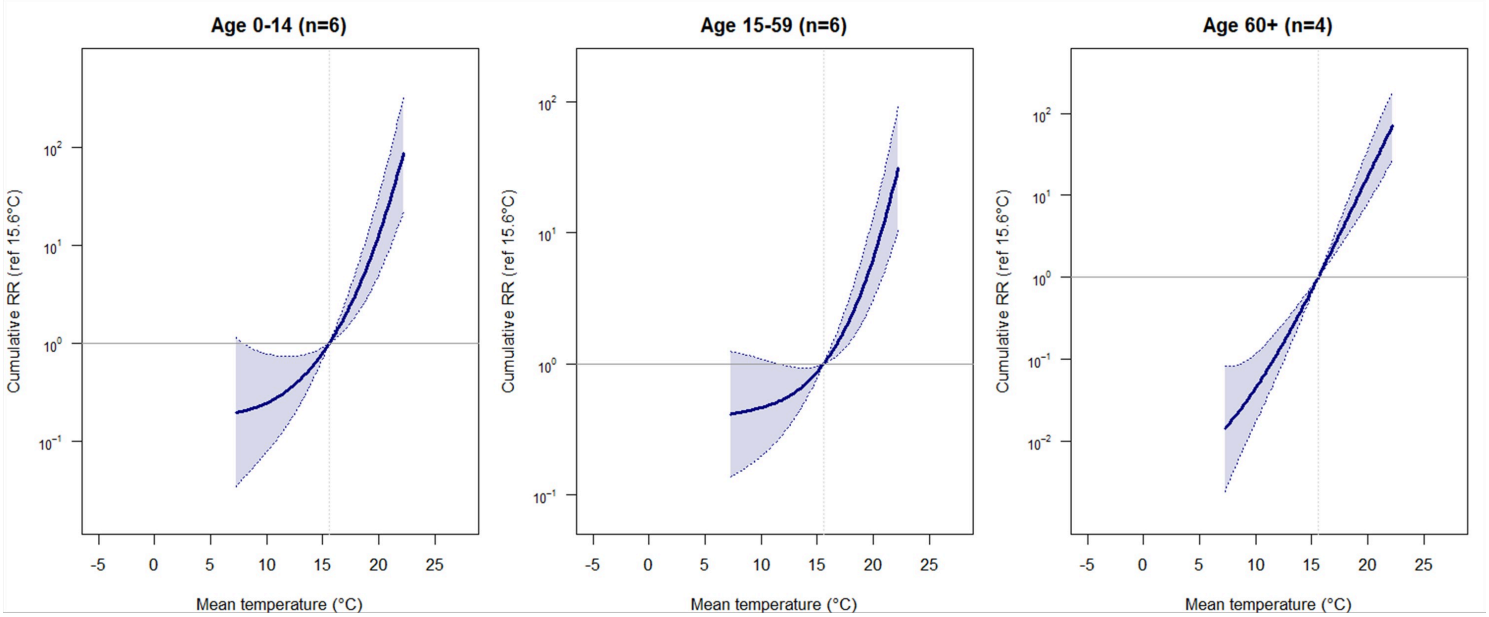


Figure 3

Pooled cumulative exposure–response curves by age band.

Curves are from multivariate meta-analysis (log scale), evaluated over the intersection of the member-series temperature ranges; shading indicates 95% CIs. The three bands show essentially identical threshold-shaped responses.

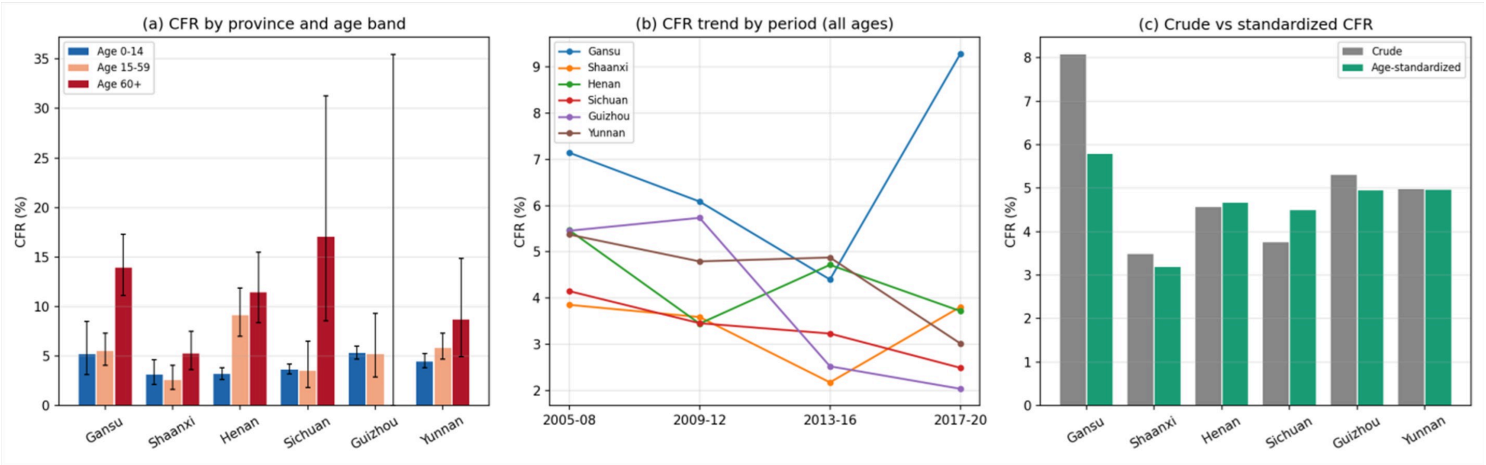


Figure 4

Case-fatality ratio (CFR) analysis.

(**A**) CFR by province and age band (Wilson 95% CIs). (**B**) CFR over four calendar periods; only Gansu rose in 2017–2020, coinciding with the adult outbreak. (**C**) Crude versus age-standardised CFR: standardisation reduces Gansu from 8.07% to 5.79%, and 94% of the Gansu–Shaanxi gap reflects age-specific rates rather than age structure.

Supplementary Files

This is a list of supplementary files associated with this preprint. Click to download.

- Supplementaryfilelegends.docx
- Additionalfile1.docx